Molecular Vision 2024; 30:175-187 <http://www.molvis.org/molvis/v30/175>
Received 27 October 2023 | Accepted 23 March 2024 | Published 25 March 2024

Phenotypic variability observed in a Chinese patient cohort with biallelic variants in the *CLN* genes

Xin Zhang, Ke Xu, Jie Shi, Yue Xie, Nien Li, Weiyu Yan, Zi-Bing Jin, Yang Li

Beijing Institute of Ophthalmology, Beijing Tongren Eye Center, Beijing Tongren Hospital, Capital Medical University, Beijing Ophthalmology & Visual Sciences Key Lab. Beijing, China

Purpose: The neuronal ceroid lipofuscinoses (NCLs) comprise a group of inherited neurodegenerative disorders with thirteen NCL-disease causing genes ceroid lipofuscinosis neuronal (*CLN)* identified. The purpose of this study was to describe the genetic and clinical characteristics of a cohort of Chinese patients harboring biallelic variants in the *CLN* genes.

Methods: We recruited 14 patients from 13 unrelated families who carried biallelic variants in the *CLN* genes. All patients underwent ophthalmic and systematic evaluations, as well as comprehensive molecular genetic analyses. Reverse transcription polymerase chain reaction (RT–PCR) assays were performed to observe the effect of a novel non-canonical splice-site (NCSS) variant on *CLN3* pre-mRNA splicing. Eventually, eight patients were followed up.

Results: We detected 21 variants in three *CLN* genes (*CLN3*, *MFSD8*, and *PPT1*); 13 variants were novel. RT–PCR assays indicated that the NCSS variant c.963–13A>G changed the pre-mRNA splicing, thereby creating an in-frame indel variant p.(W321delinsCPNLR) in *CLN3*. Diagnoses of neuronal ceroid lipofuscinosis (NCL) and non-syndromic retinal dystrophy (RD) were established in eight patients and six patients, respectively. The patients with NCL showed clinical heterogeneity, from typical phenotypes of CLN3 or CLN7 disease to juvenile- or adult-onset CLN1 disease. All patients experienced early and severe visual loss. A retinal evaluation revealed specific macular striation in 12 of the 14 patients.

Conclusions: Patients with variants in the three *CLN* genes exhibit varied clinical spectra, which might be related to their genotype. All patients presented relatively unique retinal alterations. Our findings point to a crucial need for genetic analysis for the early and accurate diagnosis of patients with NCL.

Neuronal ceroid lipofuscinoses (NCLs) comprise a group of inherited neurodegenerative disorders characterized by lysosomal accumulation of ceroid lipopigments [1,2]. Patients with NCLs usually present with retinal degeneration, dementia, motor deterioration, epilepsy, and premature death. NCLs have been classified into infantile (4–24 months), late infantile (2–5 years), juvenile (4–8 years), and adult (13–25 years) forms based on the age of symptom onset [1]. The disorders show high genetic and phenotypic heterogeneity.

Currently, 13 NCL-causing genes ceroid lipofuscinosis neuronal (*CLN*) have been identified [2]. The genes encode five lysosomal enzymes CLN1/palmitoyl-protein thioesterase 1 (*PPT1*, OMIM 600722), CLN2/tripeptidyl peptidase I (*TPP1*, OMIM 607998), *CLN5* (OMIM 608102), CLN10/cathepsin D (*CTSD*, OMIM 116840), and CLN13/cathepsin F (*CTSF*, 03539); five transmembrane proteins: CLN3 (OMIM 607042), CLN6 (OMIM 606725), CLN7/major facilitator superfamily domain-containing protein 8 (MFSD, OMIM 611124), CLN8 (OMIM 607837), and CLN12/ATPase 13A2 (ATP13A2, OMIM 610513); two cytoplasmic proteins: CLN4/DNAJ HSP40 homolog subfamily C member 5 (DNAJC5, OMIM 611203) and CLN14/potassium channel tetramerization domain-containing protein 7 (KCTD7, OMIM 611725); and one lysosome enzyme 48 chaperone: CLN11/granulin precursor (GRN, OMIM 138945). With these genes identified, NCLs are now grouped into CLN1–8 and CLN10–14 disease subtypes. All the subtypes are transmitted in an autosomal recessive pattern, with the exception of one rare adult onset CLN4 disease that is inherited in an autosomal dominant pattern [2].

CLN3 disease (OMIM 2042000), which is also known as juvenile NCL (JNCL), is the most frequent NCL subtype caused by pathogenic variants of the *CLN3* gene [3,4]. The *CLN3* gene encodes a 438 amino acid (AA) transmembrane protein involved in the transport of protons, amino acids, neurotransmitters, and proteins in lysosomes [2-4]. Typically, patients experience a rapid vision deterioration at the age of four to 10 years, followed by behavioral and cognitive dysfunction, motor decline and seizures, and ultimately death in the second decade of life [2,3].

CLN1 (OMIM 256730) and CLN7 (OMIM 610951) diseases corresponding to infantile NCL and late-infantile NCL, respectively, are caused by biallelic variants in the *CLN1* (*PPT1*) gene and *CLN7* (*MFSD8*) gene, respectively

Correspondence to: Yang Li, Beijing Institute of Ophthalmology, Beijing Tongren Hospital, Hougou Lane 17, Chong Nei Street, Beijing, 100730, China; FAX: 8610-65288561 or 65130796; Phone 8610-58265915; email: yilbio@163.com

[5-7]. The *CLN1* gene, located at chromosome 1p32, encodes a 306 AA secreted lysosomal protein, PPT1. This PPT1 enzyme is involved in the catabolism of lipid-modified proteins by the removal of fatty acids [8]. The *MFSD8* gene on chromosome 4q28.1–2 encodes a 518 AA transmembrane protein, which is likely a lysosomal transporter [7,8]. In contrast to CLN3 disease, the first symptoms in CLN1 and CLN7 phenotypes are developmental delay, followed by progressive loss of acquired psychomotor abilities, onset of epilepsy, onset of visual defect, and premature death [6-8].

Presently, more than 300 diseasing-causing variants in *PPT1*, *CLN3*, and *MFSD8* have been recorded in the Human Gene Mutation Database (HGMD) and over half of them (59%–67%) are truncating variants. Even though most of the variants are unique, some common variants show ethnic specificity. One common 1.02-kb deletion involving exons 7 and 8 of *CLN3* has been identified in 80%–85% of Caucasian patients with CLN3 disease [8-10]. Among three frequent variants in *PPT1*, two missense variants, p.Arg122Trp and p.Thr75Pro, are founder variants for patients originating from Finland and Scotland, respectively, while a nonsense variant p.Arg151X is detected in many patients of different ethnic origins [8-10].

The diagnosis of NCLs has benefited from the growing application of next-generation sequencing and has been established in more patients who exhibit a wide spectrum of phenotypes [11-15]. In contrast to the typical clinical manifestation, numerous patients with *PPT1* variants have presented with a later age of onset of NCL symptoms and a more protracted disease course, while some patients with *CLN3* or *MFSD8* variants have only shown isolated macular dystrophy or widespread retinal dystrophy (RD) [11,13,14].

In the current study, we described the clinical features of CLN-related disorders ranging from a typical syndrome manifestation to isolated RD in 14 patients from 13 unrelated families who harbor biallelic variants in one of the *CLN* genes. We also assessed the possible genotype and phenotype correlations.

METHODS

Subjects: This retrospective study was approved by the Beijing Tongren Hospital Joint Committee on Clinical Investigation, and all procedures followed the tenets of the Declaration of Helsinki. Written informed consent was obtained from all patients or their guardians. A total of 14 patients (11 males and three females) from 13 unrelated families were recruited from the Genetics Laboratory of the Beijing Institute of Ophthalmology, Beijing Tongren Eye Center, from 2012 to 2022. The inclusion criteria were that patients were clinically diagnosed with RD and harbored biallelic pathogenic or likely pathogenic variants in one of the *CLN* genes. The diagnosis of NCLs was established when patients suffered any other NCL-related neurologic manifestation.

All patients underwent thorough ocular examinations, including best-corrected visual acuity (BCVA), slit-lamp biomicroscopy, and fundus examinations. Most patients were subjected to multimodal imaging evaluations, including color fundus (CF) photography, infrared imaging (IRI), retinal spectral domain optical coherence tomography (OCT, Heidelberg, Germany), and short-wavelength fundus autofluorescence (FAF, Heidelberg, Germany). Ten patients underwent full-field electroretinography (ERG), consistent with the International Society for Clinical Electrophysiology of Vision standards.

For all patients, we documented the general medical records and systemic examination results, which involved motor function, language, intellect, and epilepsy. Some patients underwent electroencephalography (EEG) examinations and brain magnetic resonance imaging (MRI) scans. In this cohort, eight patients underwent an ophthalmic evaluation more than once, and all patients but one (067,020) participated in telephone surveys about their neurologic symptoms or signs.

Targeted exome sequencing (TES) and bioinformatics analysis: After informed consent was obtained, peripheral blood samples were collected from all participants and their available family members for genetic analysis. Genomic DNA was then extracted using a genomic DNA extraction kit (Vigorous, Beijing, China) according to the manufacturer's protocol. We performed TES in all the probands using a capture panel comprising 533 known inherited retinal disease (IRD) genes (Supplementary Table S1, including the *CLN1*-*8*, *10*, *11*, and *13* genes). The Illumina library preparation and the capture experiment were conducted as previously described [16]. The HGMD database and ClinVar database were used to search for any reported pathogenic variants.

The pathogenicity of the variants was predicted by three *in silico* programs: Mutation Taster, SIFT, and PolyPhen-2. Three algorithms, NetGene2 Server (version 2.42), NNSplice (version 0.9), and Human Splicing Finder (HSF, version 2.05), were used to analyze any variant influences on splicing. The copy number variation (CNV) kit software (https://github.com/etal/cnvkit) was utilized to detect CNVs from variations in the read depth, and real-time, quantitative polymerase chain reaction (q-PCR) was subsequently performed to confirm the existence of the presumed CNVs. Segregation analysis was performed by Sanger sequencing in all the pedigrees.

RNA extraction and analysis: A novel variant c.963–13A>G, which was identified in patient 0,191,609 and her mother and located at a non-canonical splice site (NCSS), was strongly suspected of causing aberrant splicing (Figure 1A). Fresh peripheral blood samples were obtained from patient 0,191,609 and her parents and utilized to isolate peripheral blood lymphocytes using a peripheral blood lymphocyte isolation kit (Suzhou Melian Biotechnology Co., Ltd.). Total RNA was extracted from the lymphocytes using the RNAprep Pure Cell/Bacteria Kit (Tiangong, Beijing, China). Reverse transcription PCR (RT–PCR) was performed with a pair of specific primers (forward 5′-agcccctcataagaaccgag-3′ and reverse 5′-agacgaggtagatgcttggc-3′) using the Fasting One-Step RT–PCR Kit (Tiangong Biotech, China). The products were separated by electrophoresis on 2% agarose gels, excised, and sequenced. Homology modeling of a three-dimensional (3D) structure of the CLN3 protein was generated using Swiss-Model server (https://swissmodel.expasy.org/interactive). PyMOL software was then selected to analyze the spatial conformation and stability of the predicted wild-type (WT) and mutant proteins and the hydrogen bond formation between amino acid residues.

RESULTS

NCL genes and variants: We detected 21 distinct variants of three *CLN* genes (*PPT1*, *CLN3*, and *MFSD8*) in the 13 probands. The three NCL genes were identified in the following incidences: *CLN3* in six probands, *MFSD8* in four probands, and *PPT1* in three probands. Among the 21 variants, 13 were identified in the current study. All of the novel variants were either not recorded in any public database or our in-house database or were present at a very low frequency (between 0.003% and 0.01%). All were described as pathogenic or likely pathogenic, based on the American College of Medical Genetics and Genomics (ACMG) guidelines and standards; one exception was a missense variant c.280A>C (p.T94P) in *PPT1*, which was defined as "uncertain of significance" (Table 1). This variant, which is absent from all public databases, was detected in trans with a pathogenic variant c.490C>T (p.R164X), and the retinal phenotype of proband (067,020) was similar to that of patients with *PPT1* variants. Of the 21 variants, only p.(E336K) in *MFSD8* was detected three times; the remaining 20 variants were identified only once (17/21) or twice (3/21).

Transcript analysis: The novel variant c.963–13A>G in *CLN3* was predicted to cause an abnormal splicing of exon 14 by NetGene2, NSSP, and HSF software. We then conducted further cDNA analysis to investigate the influence of this variant on *CLN3* pre-mRNA splicing. The RT–PCR results from the lymphocytes demonstrated that this novel NCSS variant caused a 12-nt retention of intron 13 (Figure 1B, C), resulting in an in-frame indel p.(W321delinsCPNLR) by triggering a cryptic acceptor splice site. The 3D structural modeling demonstrated that the mutant changed one segment of an α-helical secondary structure to a loop structure (Figure 1D). The bioinformatic analysis predicted that the mutant altered the lengths and angles of several hydrogen bonds between the related residues (Figure 1D).

Clinical findings: In the current cohort, six probands, four probands, and four patients from three unrelated pedigrees harbored compound heterozygous variants in *CLN3*, *MFSD8*, and *PPT1*, respectively. All the variants were verified by familial segregation analyses (Supplement Figure 1). Of the 14 patients, eight were diagnosed with NCLs and six were diagnosed with isolated RD. All the patients experienced night blindness or different extents of vision defect and were initially diagnosed with retinitis pigmentosa (RP, seven patients) or cone-rod dystrophy (CORD, seven patients; Table 2).

Of the six probands carrying biallelic *CLN3* disease-causing variants, five were diagnosed with NCL and one was diagnosed with isolated RP. The five patients with NCL presented typical clinical features of CLN3 disease, and their mean age at last examination was 9.8 years (range: 7.0–15.3 years). These patients suffered a rapid visual defect, mostly combined with nyctalopia, followed by a neurologic manifestation, which included intellect and language function decline, motor ability defect, and epileptic seizure. The mean onset age for visual loss was 6.4 years (range: 6–8 years), while the mean onset age for neurologic symptoms was 8.8 years (range: 7–12 years). In contrast, patient 019,309 with isolated RP, whose last exam age was 31.4 years, had a late onset age (16 years) for his ocular symptoms. He had not developed any neurologic symptoms at his latest telephone follow-up at the age of 42.

The four probands with biallelic *MFSD8* variants were clinically diagnosed with CORD, and their mean onset age for ocular symptoms was 8.1 years (range: 5–13.5 years). In addition to the ocular symptoms, proband 010,421 simultaneously suffered mental retardation and epileptic seizure at the age of five, followed by the development of speech impairment at age eight and then paralysis and bedridden in what resembled a vegetative state at the age of 12 at his most recent telephone follow-up. His brain MRI at age 12 revealed obvious cerebellar atrophy.

Of the four patients carrying biallelic *PPT1* variants, two had a neurologic manifestation and two had only RD at their last examination (3.5 years and 15.8 years, respectively). All

four patients suffered visual defect with night blindness, and their mean onset age was 8.9 years (range: 0.5–15 years). None of the four patients presented any typical clinical features of CLN1 disease. Proband 010,707 (11.5-year-old male) had suffered only mild mental retardation at the age of eight, while proband 019,953 (25.2-year-old female) had developed hypomnesia, mild dysarthria, emotional instability, and motor ability deterioration at the age of 24. Her brain MRI displayed whole-brain atrophy at her last examination. Her younger brother 019,953-3 (15.8 years old) only presented with rapid visual defects with night blindness.

Ophthalmic features: The 14 patients presented profound visual loss with a mean logMAR BCVA of 1.4 (range: 0.4–2.7), and eight of them experienced a rapid visual decline over 3–6 months. Nystagmus was observed in one patient (010,421). Among the 10 patients whose ERG recordings were available, four displayed severe dysfunction in rod and cone responses, three showed extinguished rod responses and severe dysfunction in cone responses, and three exhibited an extinguished recording (Table 2).

Retinal features: Fundus examinations revealed that all 14 patients exhibited macular alteration ranging from bull's eye maculopathy to total macular atrophy, arteriolar attenuation,

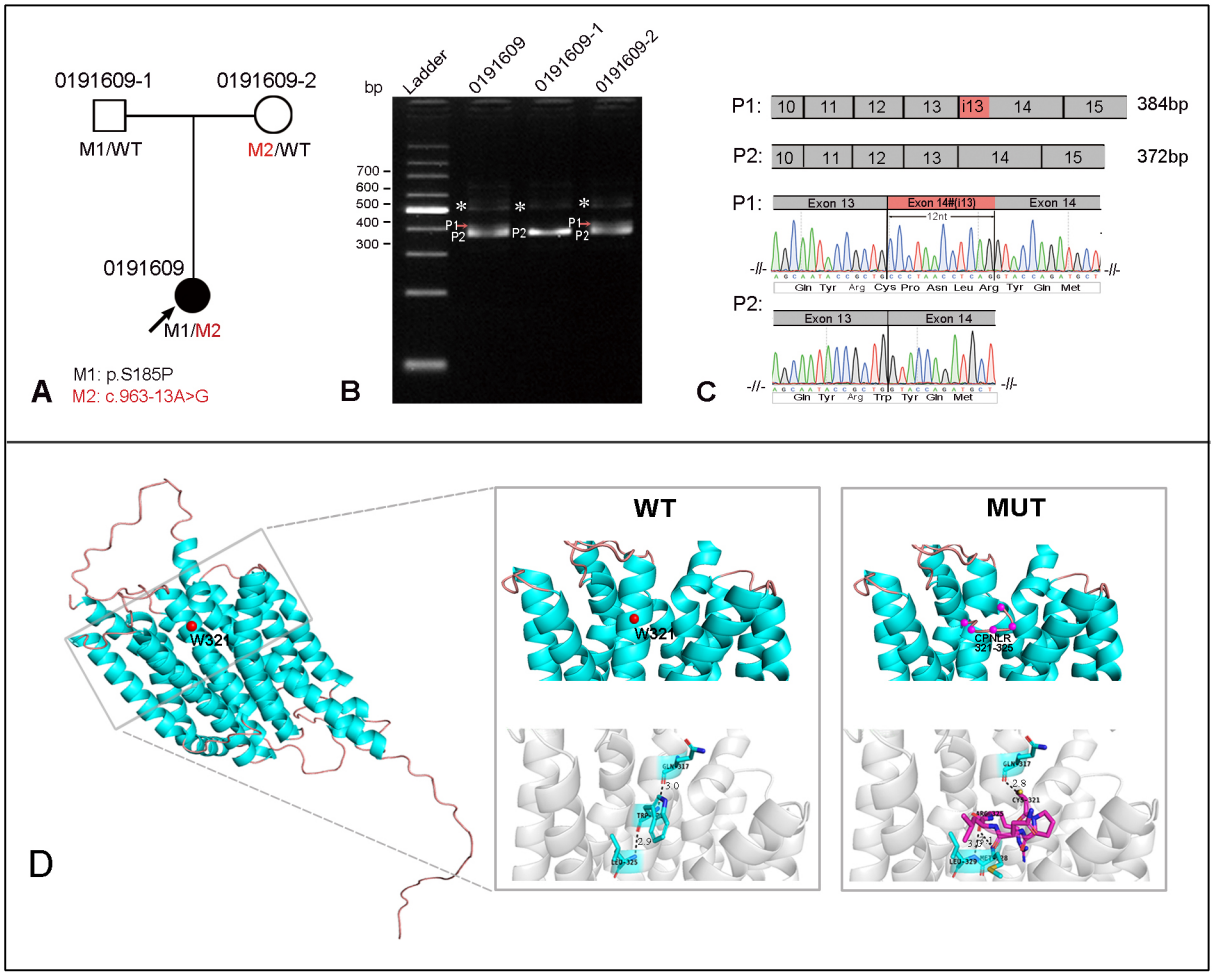

Figure 1. Pedigree, co-segregation, and the reverse transcriptase (RT)–PCR analysis for a novel variant c.963–13A>G in *CLN3* in proband 0,191,609. **A** Pedigree and segregation analysis results. **B** RT–PCR analysis revealed an abnormal band (P1, red arrow) and a wild-type (WT) band (P2) in the proband and her mother, while her father showed only a WT band. Asterisks denote fragments for which no sequence information was obtained. **C** Schematic representation and partial sequence chromatogram of P1 containing 12-nt retention of intron 13(i13). **D** The Predicted 3D protein structures of CLN3 in the WT and mutant (MUT). One segment of α-helical secondary structures that involved residue W321 (red dot) in the WT was replaced by a loop structure (in purple) in the MUT. The dotted lines indicated the hydrogen bonds between the residues. The number represented the lengths of the hydrogen bonds.

Table 1. Pathogenic variants identified in this study and analysis of the variants by predictive programs.

Gene	Exon	Nucleotide Changes	Amino Acid Changes	Variant type	Allele	MT	PP2	SIFT	NG2	NNSP	HSF	In-house	MAF	ACMG	ClinVar ID
PPT1	1	c.24G>A	p.(W8X)	NS	1	DC	-	-	-	-	-	-	-	LP	novel
PPT1	3	c.280A>C	p.(T94P)	MS	1	PO	B	T	N	N	N	-	-	U	novel
PPT1	3	c.338G>T	p.(G113V)	MS	1	DC	PD	D	N	N	N	-	-	LP	novel
PPT1	3	c.348G>C	p.(Q116H)	MS	1	DC	PD	D	N	N	N	-	-	LP	novel
PPT1	5	c.490C>T	p.(R164X)	NS	1	DC	-	-	-	-	-	-	0.0001	P	56,197
PPT1	6	c.595A>G	p.(S199G)	MS	1	DC	PD	D	-	-	-	-	-	LP	novel
CLN3	4	c.206C>A	p.(S69X)	NS	1	DC	-	-	-	-	-	-	-	LP	novel
CLN3	9	c.553T>C	p.(S185P)	MS	1	DC	PD	D	N	N	N	0.00022	0.00022	LP	novel
CLN3	12	c.838G>T	p.(G280C)	MS	1	DC	PD	D	SC	N	N	-	-	LP	novel
CLN3	12	c.906+5G>A	p.(?)	SP	2	-	-	-	SC	SC	SC	-	-	LP	56,291
CLN3	13	c.962+1G>A	p.(?)	SP	1	DC	-	-	SC	SC	SC	0.00022	0.00022	P	370,144
CLN3	14	c.963–13A>G	p.(W321delinsCPNLR)	SP	1	-	-	-	SC	SC	SC	-	-	LP	novel
CLN3	14	c.976dupT	p.(Y326Lfs*56)	FS	1	DC	-	-	-	-	-	-	-	LP	novel
CLN3	14	c.1001G>A	p.(R334H)	MS	2	DC	PD	D	N	N	N	-	0.00002407	P	56,244
CLN3	15	e15–16del	p.(?)	CNV	1	-	-	-	-	-	-	-	-	P	novel
CLN3	16	c.1213C>T	p.(R405W)	MS	1	DC	PD	D	N	N	N	-	0.00003298	LP	418,137
MFSD8	11	c.1006G>A	p.(E336K)	MS	3	DC	PD	D	N	N	N	-	0	LP	284,230
MFSD8	12	c.1268C>G	p.(A423G)	SP	1	PO	B	T	SC	SC	SC	-	-	LP	novel
MFSD8	12	c.1345_1346del	p.(P449Sfs*72)	FS	1	DC	-	-	-	-	-	-	-	LP	novel
MFSD8	13	c.1351–1G>A	p.(?)	SP	2	-	-	-	SC	SC	SC	0.00022	0.0001	LP	1,180,775
MFSD8	13	c.1391C>T	p.(A464V)	MS	1	DC	PD	D	N	N	N	-	0	LP	1,004,070

Ref_Transcript: *PPT1*:NM_000310; *CLN3*:NM_001042432; *MFSD8*:NM_152778. Abbreviations: ACMG, classification of variants according to American College of Medical Genetics; B, benign; CNV, copy number variant; D, Damaging; DC, Disease causing; e, exon; FS, frameshift; HSF, Human Splicing Finder; IF, in-frame; LP, likely pathogenic; MAF, minor allele frequency; MS, missense; MT, Mutation Taster; N, no change; NNSP, NNSplice; NG2, NetGene2; NS, nonsense; P, pathogenic; PD, possible deterioration ; PO, polymorphism; PP2, Polyphen2; SC, Splice site changed; SP, Splice; T, tolerant; U, uncertain of significant.

Table 2. The clinical features and follow-up informations of 14 patients with *CLN* genes.

Patient ID	Gender	Onset age (year)	Exam age (year)		BCVA LogMAR (OD/OS)		First symptoms	Macular alteration	ERG	Neurobehavioral symptom (onset age, year)					*Gene*	Variants
			First	Last	First	Last				I	L	MF	EP	Others		
067,020	Male	0.5	NA	3.5	NA	NA	VL	MA, MS	NA	No	No	No	No	No	*PPT1*	p.R164X/p.T94P
010,707*	Male	7	NA	11.5	NA	2.3/2.3	VL, NB	MA, MS	rod:E; cone:SD	8	No	No	No	No	*PPT1*	p.G113V/p.Q116H
019,953	Female	13	19.3	25.2	1.3/1	2.7/2.7	NB, VL	MA, MS	rod:E; cone:SD	24	25	25	No	SB, brain atrophy	*PPT1*	p.W8X/p.S199G
019,953-3	Male	15	NA	15.8	NA	0.4/0.4	RVL, NB	MD, TD	rod:E; cone:SD	No	No	No	No	No	*PPT1*	p.W8X/p.S199G
019,309	Male	16	NA	31.4	NA	1/2.3	NB, VL	MA, MS	NA	No	No	No	No	No	*CLN3*	p.S69X/p.R405W
0,191,609	Female	8	8.8	11.2	2.3/2.7	3.0/2.7	RVL, NB	MA, MS	E	11	11	No	No	N&NT, EEG-ab(11)	*CLN3*	p.S185P/c.963–13A>G
0,191,730	Male	6	7.1	7.3	1.85/1.85	1.85/1.85	RVL	MA, MS	SD	7	7	No	No	EEG-ab(7)	*CLN3*	c.962+1G>A/e15–16del
0,191,773	Male	6	6.5	8.6	1/1	1.7/1.7	NB, RVL	BM to MA&MS	E	7	8	8	No	bipolar disorder	*CLN3*	p.G280C/p.Y326Lfs*56
010,769*	Male	6	6.6	7.0	1.7/1.7	2.0/2.0	RVL, NB	BM to MA&MS	SD	7	7	No	No	No	*CLN3*	p.R334H/c.906+5G>A
010,272*	Male	6	7.3	15.3	1.22/1.4	2.7/2.7	RVL, NB	MA, MS	SD	12	15	15	10	N&NT(5)	*CLN3*	p.R334H/c.906+5G>A
010,124*	Male	6	NA	7.3	NA	2.3/2.3	VL, NB	MA, MS	E	No	No	No	No	No	*MFSD8*	p.P449Sfs*72/p.A423G
010,421*	Male	5	NA	6	NA	1.1/1.1	RVL, nystagmus	MA, MS	NA	5	(#8)	(#10)	5	bedridden &CA (#12)	*MFSD8*	c.1351–1G>A/p.A464V
010,777*	Female	8	9.1	11.0	0.4/1	1.3/1.3	VL	BM	SD	No	No	No	No	No	*MFSD8*	c.1351–1G>A/p.E336K
010,962*	Male	13	13.5	20.4	0.82/0.92	1.52/1.52	RVL	MA, MS	NA	No	No	No	No	No	*MFSD8*	p.E336K/p.E336K

Abbreviations: BA, brain atrophy; BM, bull's eye maculopathy; BCVA, best corrected visual acuity; CA, cerebellar atrophy; E,extinguish; e,exon; EEG-ab, electroencephalograph abnormal; EP, Epilepsy; I, Intellect decline; L, language function decline; MA, macular atrophy; MD, macular edema; MF, Motor function defect; MS, macular striation; NB, night blindness; N&NT, nightmares and night terrors; OD, right eye; OS, left eye; RVL, rapid vision loss; SB, sinus bradycardia; SD, severe decline; VL,vision loss. *, patients diagnosed with cone-rod dystrophy. (#), Information obtained by telephone follow-up.

and tapetoretinal degeneration (TD) in the mid-peripheral retina (Figure 2, Figure 3, and Figure 4). A distinctive radial macular striation was observed in 12 of 14 patients (86%; Figure 2; Figure 3A–B, D; and Figure 4A, C). The two exceptions were patient 010,777 (Figure 3C) and patient 019,953-3 (Figure 4B), who carried variants in *MFSD8* and *PPT1,* respectively. The linear striations were easily observed by IR imaging (Figure 2A,B). In addition, optic disc pallor was detected in 11 patients (Figure 2, Figure 3, and Figure 4). FAF examination showed an enlarged area of hypo-autofluorescence (AF) in the foveal region surrounded by an area of hyper-AF in the posterior pole (Figure 2A,B; Figure 3C,D; and Figure 4). Several cases displayed patchy hypo-AF in the midperiphery and along the arcades (Figure 4A,B). Retinal OCT scans were available for analysis in 10 patients. OCT images of all the cases showed macular atrophy with almost total loss of the ellipsoid zone (EZ) in the macula and paramacular regions (Figure 2A–D; Figure 3B–D; Figure 4A,C). The one exception was patient 019,953-3, who showed bilateral macular edema (Figure 4B). Numerous hyperreflective substances were observed at the level of the retinal pigment epithelium (RPE) in all eyes. With the exception of patient 019,953-3 and patient 010,777, all the cases showed fine rippling at the level of the internal limiting membrane, which correspond to the macular striation observed by CF and IR.

Longitudinal observation of eight follow-up patients: We followed eight patients for their ocular longitudinal changes for a mean follow-up time of 42 months (range: 3–96 months). During follow-up, seven patients presented a severely decreased BCVA, as their mean logMAR BCVA at the first exam time was 1.32 (range: 0.4–2.7), while the mean logMAR BCVA at the last exam time was 2.1 (range: 1.3–3.0). The one remaining patient 0,191,730 showed a stable BCVA but had only a three-month follow-up. Our fundus evaluations revealed different extents of progression of retinal degeneration in all the patients, with features that included enlargement of macular atrophy, expanded retinal and RPE atrophy, and the occurrence of optic pallor and vascular attenuation with aging (Figure 2, Figure 3, and Figure 4). The OCT scans disclosed obviously increasing hyperreflective dots at the RPE level even during a short three-month follow-up (Figure 2A). In addition, the normal retinal lamination vanished, and the fine macular striation decreased with aging (Figure 2D and Figure 4A).

DISCUSSION

In this study, we performed comprehensive genetic analyses in a small Chinese cohort from a tertiary center. We depicted the genetic and clinical features of the 14 patients with biallelic variants in *CLN3*, *MFSD8,* and *PPT1* and characterized the retinal phenotype of these patients.

Of the 21 variants in the three *CLN* genes, 13 were initially identified in the current cohort. This cohort also contained none of the reported common variants, such as the 1.02 kb deletion in *CLN3*. Moreover, these common variants have not been described in any previous Chinese studies [17-23]. Collectively, these findings indicated that the variant spectrum for each of the three genes for Chinese patients differed from the spectra described in other populations. The 10 variants in *CLN3* included three splicing site variants and one large deletion variant. Two of the three splicing site variants were located at the NCSS. Our RT–PCR analysis revealed that the novel c.963–13A>G caused an abnormal splicing product that stimulated a cryptic splice acceptor site. The abnormal splicing product contained a 12-nt retention of intron 13, which did not disturb the open reading frame. As the incorporation of additional four amino acids altered the 3D structure of the protein, we speculated that this novel NCSS variant might impact the function of the protein. Our results further indicated the significance of investigating the noncoding region or CNVs when conducting genetic analysis.

The patients in our cohort displayed variable expressivity of the phenotype, which might be related to their genotypes. Consistent with a previous description of patients with *CLN3* variants [24], the eight patients with NCLs presented only ocular symptoms or signs as their initial clinical manifestation at an early stage, which might have caused a delay in their diagnosis of NCLs. For the five probands who carried compound heterozygous variants, one truncating variant (nonsense, frameshift indel, or splicing-site variants) was combined with one missense variant in *CLN3*. Four patients presented a typical CLN3 disease phenotype, whereas the remaining patient, 019,309, who harbored a heterozygous missense variant p.R405W, suffered only isolated RP. Compared to the patients with CLN3 disease, patient 019,309 had a later onset age and a relatively mild visual defect. In a recent study, four of five patients with biallelic variants in *CLN3* presented with isolated RP, and these four patients harbored either a homozygous missenses variant (p.E295G or p.A59T) or a heterozygous p.R405W combined with the common 1.02-kb deletion [13]. The p.R405W variant has been identified in several cases with isolated RP, either in a homozygous state or a heterozygous state combined with the 1.02-kb deletion [11]. However, one Iraqi patient with

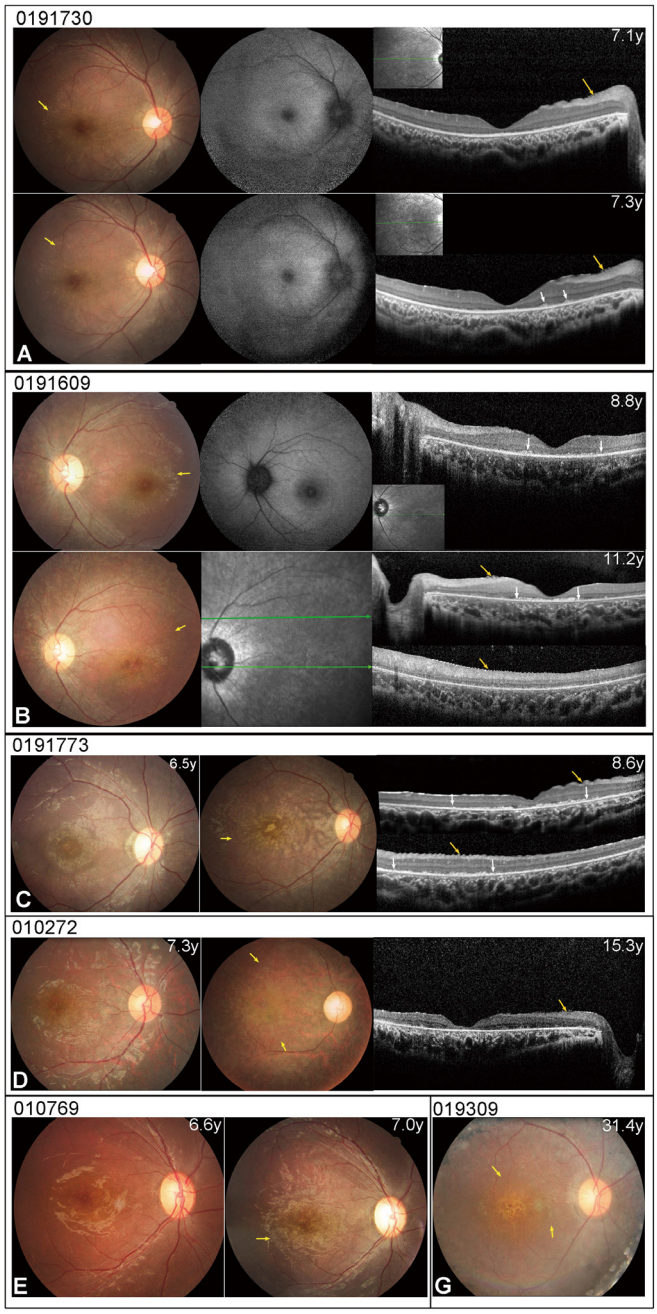

Figure 2. CF, FAF, IRI, and OCT images of patients carrying *CLN3* variants. **A-G**: CF images showed macular atrophy, macular striation, and retinal degeneration (RD) in all the patients. OCT scans in four patients revealed a diffuse loss of the outer retinal structure and hyper-reflective remnants in the upper retinal pigment epithelium (RPE) level (white arrows). Macular striation (yellow arrows) showed as fine rippling on OCT scans, corresponding to linear striations in the CF and IRI. FAF displayed hyper-AF in the posterior pole surrounded by hypo-AF in the midperiphery. In follow-up examinations, OCT scans revealed increases in the hyperreflective substances in patient 0,191,730 and patient 0,191,609 (**A** and **B**, respectively). The CF photographs of patient 0,191,773 and patient 010,769 showed radial macular striation only at the last visit (**C** and **E**, respectively). The CF photograph of patient 010,272 exhibited decreased macular striation after eight years of follow-up **(D)**.

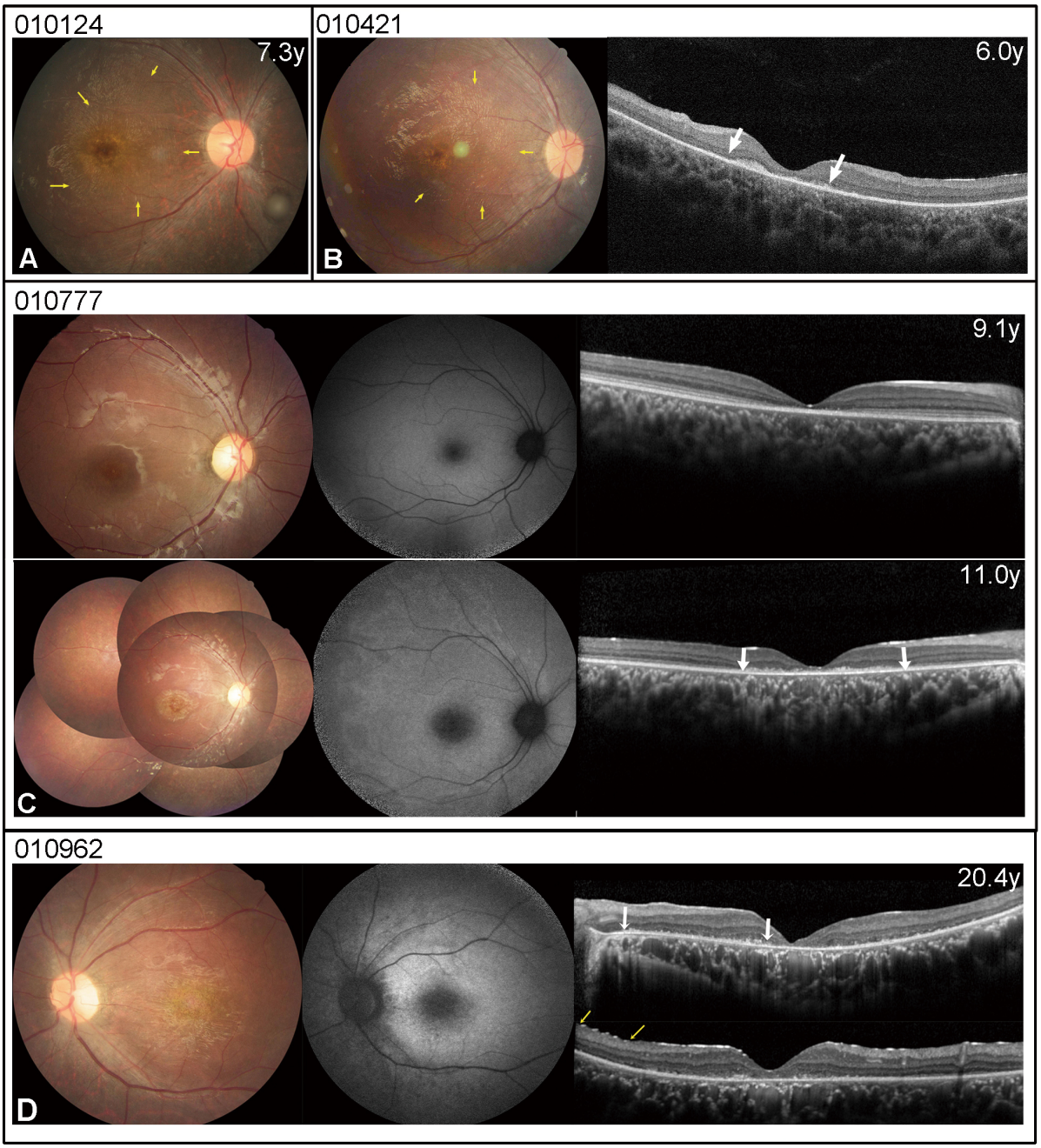

Figure 3. CF, FAF, and OCT) images of patients harboring variants in *MFSD8* genes. **A, B,** and **D**: CF photographs of patient 010,124, patient 010,421, and patient 010,962, respectively, displayed macular atrophy, macular striation (yellow arrows), and diffuse retinal degeneration (RD). **C** CF of patient 010,777 showed bull's eye maculopathy, and OCT revealed macular atrophy. During her two years of follow-up, CF and OCT images revealed advanced macular atrophy and hyperreflective substances (white arrows) in the macular region, while FAF showed expansion of the enlarged area of hypo-AF in the foveal region.

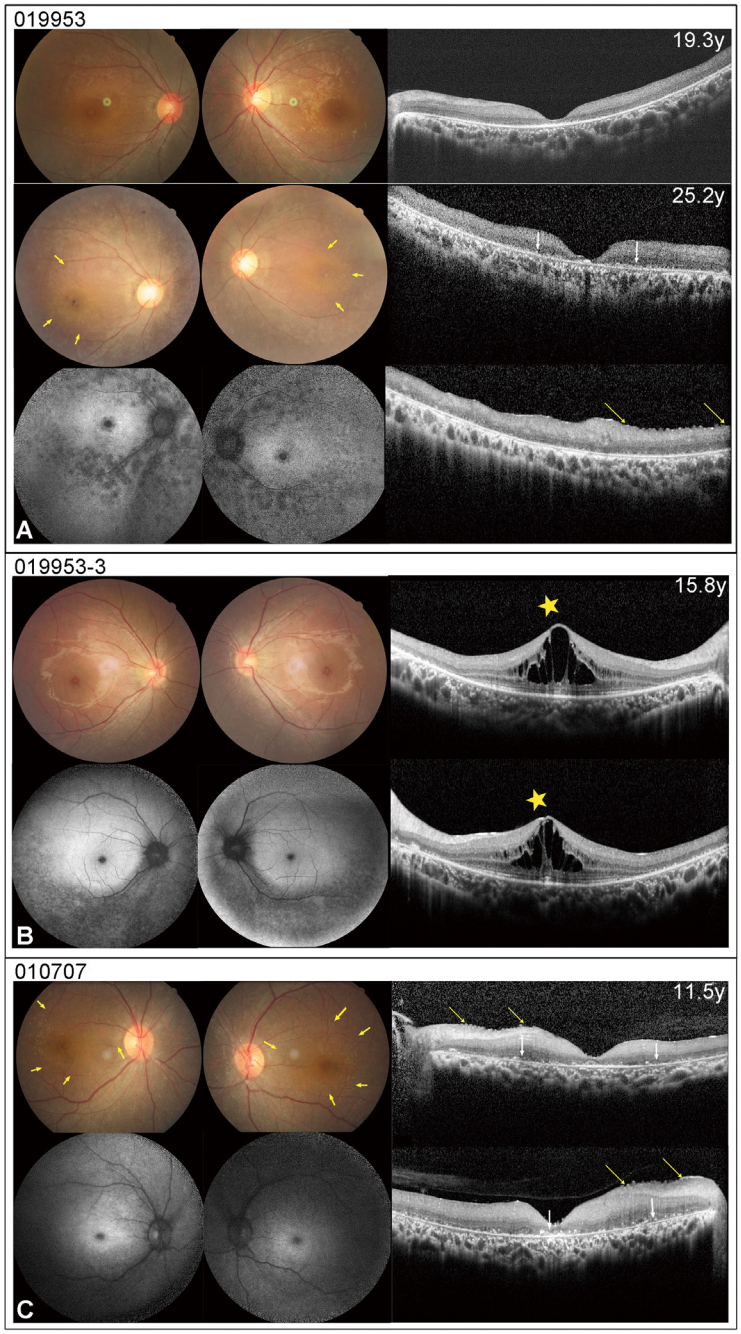

Figure 4. CF photographs, FAF, and OCT images of three patients carrying *PPT1* variants. **A** CF image of patient 019,953 showed a blunted foveal reflex and mild retinal degeneration (RD) in the peripheral retina, while her OCT scan displayed macular atrophy at the age of 19.3 years. Her CF and OCT images indicated macular striation (yellow arrows), a total loss of ellipsoid zone, and hyper-reflective dots in the RPE level (white arrow) at the age of 25.2 years. Her FAF displayed an enlarged area of hypo- AF area in the foveal region, surrounded by a hyper-AF region in the posterior pole and a patchy hypo-AF region in the midperipheral retina. **B** CF and OCT of patient 019,953-3 showed marked macular edema (yellow asterisk) and peripheral RD. His FAF appearance was similar to that of his sister (patient 019,953). **C** CF, OCT, and FAF images of patient 010,707 disclosed a fundus appearance akin to that observed in patient 019,953 at the age of 25.2 years.

homozygous p.R405W initially diagnosed with isolated RP at the age of 20 developed neurologic symptoms or signs at the age of 30 [25].

Among the four patients with *MFSD8* variants, two patients (010,421 and 010,777) carried the same heterozygous splicing-site variant c.1351–1G>A, but it was combined with a missense variant p.A464V or p.E336K. The patient carrying c.1351–1G>A/p.A464V presented a relatively typical CLN7 disease phenotype, while the patient harboring c.1351–1G>A/p.E336K only displayed isolated CORD, which was also observed in another patient (010,962) who carried a homozygous p.E336K. The variant p.A464V was initially identified in a Chinese family that included two patients with CLN7 disease [19]. In contrast, variant p.E336K was detected in several patients with isolated macular dystrophy when paired either with a truncating variant or a missense variant [14]. Therefore, p.E336K might be considered a "mild" allele, while p.A464V might be considered a "severe" allele. The two patients with variants in *PPT1* suffered neurologic manifestations, as patient 010,707 with compound heterozygous variants p.G113V/p.Q116H showed a juvenile onset age (eight years of age), while patient 019,953 with p.W8X/p.S199G presented an adult onset age (24 years of age) for their neurologic problems. The pathogenic role of the *PPT1* variants is related to the resultant reduction in enzyme activity, with biallelic truncating variants usually resulting in an infantile onset phenotype [8]. The variant p.S199G might produce a milder deleterious effect than variants p.G113V and p.Q116H, whose locations were close to residue p. S115, the first catalytic triad of PPT1 [8].

Consistent with previous observations, more than half of the patients in the current cohort experienced rapid vision loss, which was more common in patients with *CLN3* variants [26]. Moreover, the visual defects rapidly progressed in our follow-up observation, which was different than our previous findings noted in patients with other IRDs [27,28]. Our retinal evaluation revealed that all 14 patients had macular alterations, and 12 of them presented the characteristic macular striation, which was observed and described in patients with variants in *CLN3* [13,24,26]. We found that patients with variants in *MFSD8* and *PPT1* also had a fine macular striation, which can decrease with disease progression during longitudinal observation. Dulz et al. speculated that the macular alteration resulted from a pathological degenerative or secondary inflammatory process in the internal limiting membrane and the nerve fiber layer at the macular region [26]. The two patients who did not have macular striations were in the early stage of disease. This finding was also similar to previous observations in patients with variants in *CLN3* [13,24,26]. The current study has several limitations, including a retrospective design, small number of patients, and incomplete neurologic evaluation for some patients.

In conclusion, our study has expanded the variant spectra for *CLN3*, *MFSD8*, and *PPT1*. Patients with variants in the three *CLN* genes exhibited varied clinical spectra, which might be related to their genotypes. All the patients presented relatively unique retinal alterations. Our findings reveal a crucial need for genetic analysis for the early and accurate diagnosis of patients with NCLs.

APPENDIX 1. SUPPLEMENTARY TABLE 1.

To access the data, click or select the words "Appendix 1." The list of Genes of the inherited retinal degeneration gene capture panel in this study.

APPENDIX 2. SUPPLEMENTARY FIGURE 1.

To access the data, click or select the words "Appendix 2." Pedigrees and co-segregation of all families.

ACKNOWLEDGMENTS

This study was supported by the National Key R&D Program of China (2022YFC2703600). The funding organizations had no role in designing or conducting this research. Financial support: This work was supported by the National Key R&D Program of China, 2022YFC2703600. The funding organization had no role in the design or conduct of this research. Conflict with interest: No authors have any financial/conflicting interests to disclose.

REFERENCES

1. Mole SE, Cotman SL. Genetics of the neuronal ceroid lipofuscinoses (Batten disease). Biochim Biophys Acta 2015; 1852:10 Pt B2237-41. [PMID: 26026925].
2. Specchio N, Ferretti A, Trivisano M, Pietrafusa N, Pepi C, Calabrese C, Livadiotti S, Simonetti A, Rossi P, Curatolo P, Vigevano F. Neuronal Ceroid Lipofuscinosis: Potential for Targeted Therapy. Drugs 2021; 81:101-23. [PMID: 33242182].
3. Phillips SN, Benedict JW, Weimer JM, Pearce DA. CLN3, the protein associated with batten disease: structure, function and localization. J Neurosci Res 2005; 79:573-83. [PMID: 15657902].
4. Shematorova EK, Shpakovski GV. Current Insights in Elucidation of Possible Molecular Mechanisms of the Juvenile Form of Batten Disease. Int J Mol Sci 2020; 21:8055-[PMID: 33137890].
5. Mole SE, Anderson G, Band HA, Berkovic SF, Cooper JD, Kleine Holthaus S-M, McKay TR, Medina DL, Rahim AA,

Schulz A, Smith AJ. Clinical challenges and future therapeutic approaches for neuronal ceroid lipofuscinosis. Lancet Neurol 2019; 18:107-16. [PMID: 30470609].

6. Augustine EF, Adams HR, de Los Reyes E, Drago K, Frazier M, Guelbert N, Laine M, Levin T, Mink JW, Nickel M, Peifer D, Schulz A, Simonati A, Topcu M, Turunen JA, Williams R, Wirrell EC, King S. Management of CLN1 Disease: International Clinical Consensus. Pediatr Neurol 2021; 120:38-51. [PMID: 34000449].

7. Kousi M, Siintola E, Dvorakova L, Vlaskova H, Turnbull J, Topcu M, Yuksel D, Gokben S, Minassian BA, Elleder M, Mole SE, Lehesjoki A-E. Mutations in CLN7/MFSD8 are a common cause of variant late-infantile neuronal ceroid lipofuscinosis. Brain 2009; 132:810-9. [PMID: 19201763].

8. Kousi M, Lehesjoki A-E, Mole SE. Update of the mutation spectrum and clinical correlations of over 360 mutations in eight genes that underlie the neuronal ceroid lipofuscinoses. Hum Mutat 2012; 33:42-63. [PMID: 21990111].

9. Mole SE. The genetic spectrum of human neuronal ceroid-lipofuscinoses. Brain Pathol 2004; 14:70-6. [PMID: 14997939].

10. Adams HR, Beck CA, Levy E, Jordan R, Kwon JM, Marshall FJ, Vierhile A, Augustine EF, de Blieck EA, Pearce DA, Mink JW. Genotype does not predict severity of behavioural phenotype in juvenile neuronal ceroid lipofuscinosis (Batten disease). Dev Med Child Neurol 2010; 52:637-43. [PMID: 20187884].

11. Ku CA, Hull S, Arno G, Vincent A, Carss K, Kayton R, Weeks D, Anderson GW, Geraets R, Parker C, Pearce DA, Michaelides M, MacLaren RE, Robson AG, Holder GE, Heon E, Raymond FL, Moore AT, Webster AR, Pennesi ME. Detailed Clinical Phenotype and Molecular Genetic Findings in CLN3-Associated Isolated Retinal Degeneration. JAMA Ophthalmol 2017; 135:749-60. [PMID: 28542676].

12. Ozono T, Kinoshita M, Narita A, Hirakiyama A, Kosuga M, Okuyama T, Fukada K. Juvenile-onset neuronal ceroid lipofuscinosis (CLN1) disease with a novel deletion and duplication in the PPT1 gene. J Neurol Sci 2018; 388:4-6. [PMID: 29627028].

13. Kolesnikova M, Lima de Carvalho JR Jr, Oh JK, Soucy M, Demirkol A, Kim AH, Tsang SH, Breazzano MP. Phenotypic Variability of Retinal Disease Among a Cohort of Patients With Variants in the CLN Genes. Invest Ophthalmol Vis Sci 2023; 64:23-[PMID: 36912596].

14. Priluck AZ, Breazzano MP. Novel *MFSD8* mutation causing non-syndromic asymmetric adult-onset macular dystrophy. Ophthalmic Genet 2023; 44:186-90. [PMID: 35801630].

15. Panjeshahi S, Karimzadeh P, Movafagh A, Ahmadabadi F, Rahimian E, Alijanpour S, Miryounesi M. Clinical and genetic characterization of neuronal ceroid lipofuscinoses (NCLs) in 29 Iranian patients: identification of 11 novel mutations. Hum Genet 2023; 142:1001-16. [PMID: 37074398].

16. Sun T, Xu K, Ren Y, Xie Y, Zhang X, Tian L, Li Y. Comprehensive Molecular Screening in Chinese Usher Syndrome Patients. Invest Ophthalmol Vis Sci 2018; 59:1229-37. [PMID: 29625443].

17. Bi HY, Yao S, Bu DF, Wang ZX, Zhang Y, Qin J, Yang YL, Yuan Y. [Two novel mutations in palmitoyl-protein thioesterase gene in two Chinese babies with infantile neuronal ceroid lipofuscinosis] Zhonghua Er Ke Za Zhi 2006; 44:496-9. [PMID: 17044973].

18. Lau NKC, Ching CK, Lee HHC, Chak WKM, Kwan Shing N, Hanchard NA, Mak CM. First case of genetically confirmed CLN3 disease in Chinese with cDNA sequencing revealing pathogenicity of a novel splice site variant. Clin Chim Acta 2018; 486:151-5. [PMID: 30053402].

19. Chen XY, Zhu YJ, Mei DQ, Mei SY, Wang L, Ma YL, Chen GH, Zhang YD. MFSD8 gene mutation and clinical characteristics of a family with neuronal ceroid lipofuscinosis type 7. Zhonghua Yi Xue Yi Chuan Xue Za Zhi 2023; 40:395-401. .

20. Zeng SJ, Liu T, Wang LS, Yang L, Cheng GQ, Qiu HX. Clinical characteristics of a family with one case neuronal ceroid lipofuscinosis type 7 occurred in neonatal and literature review. Chin Pediatr Emerg Med 2021; 28:723-6. .

21. Qiao Y, Gu Y, Cheng Y, Su Y, Lv N, Shang Q, Xing Q. Case Report: Novel MFSD8 Variants in a Chinese Family With Neuronal Ceroid Lipofuscinoses 7. Front Genet 2022; 13:807515[PMID: 35154277].

22. He S, Chen S, Peng Y, Fan X, Li S, Zhang J. [Clinical characteristics and genetic analysis of a case with adult neuronal ceroid lipofuscinosis type 7 due to variant of MFSD8 gene] Zhonghua Yi Xue Yi Chuan Xue Za Zhi 2023; 40:395-401. [PMID: 36972931].

23. Ren SCGB, Gao BQ, Wang YJ, Wu XJ, Tian ZX, Sun YL. [Clinical, genetic and pathological features of neuronal ceroid lipofuscinosis in 5 Chinese patients] Zhonghua Yi Xue Za Zhi 2016; 96:3504-7. [PMID: 27903347].

24. Wright GA, Georgiou M, Robson AG, Ali N, Kalhoro A, Holthaus SK, Pontikos N, Oluonye N, de Carvalho ER, Neveu MM, Weleber RG, Michaelides M. Juvenile Batten Disease (CLN3): Detailed Ocular Phenotype, Novel Observations, Delayed Diagnosis, Masquerades, and Prospects for Therapy. Ophthalmol Retina 2020; 4:433-45. [PMID: 31926949].

25. Kuper WFE, van Alfen C, van Eck L, van den Broek BTA, Huisman A, van Genderen MM, van Hasselt PM. A Case of Unexpected Adult-Onset Neurologic Decline in CLN3-Associated Retinal Degeneration. JAMA Ophthalmol 2017; 135:1451-3. [PMID: 29049447].

26. Dulz S, Wagenfeld L, Nickel M, Richard G, Schwartz R, Bartsch U, Kohlschütter A, Schulz A. Novel morphological macular findings in juvenile CLN3 disease. Br J Ophthalmol 2016; 100:824-8. [PMID: 26486417].

27. Song Y, Chen C, Xie Y, Sun T, Xu K, Li Y. Clinical and genetic findings in a Chinese cohort with choroideremia. Eye (Lond) 2023; 37:459-66. [PMID: 35132212].

28. Shi J, Xu K, Hu JP, Xie Y, Zhang X, Zhang XH, Jin ZB, Li Y. Clinical Features and Natural History in a Cohort of Chinese Patients with RPE65-Associated Inherited Retinal Dystrophy. J Clin Med 2021; 10:5229-[PMID: 34830511].

Articles are provided courtesy of Emory University and the Zhongshan Ophthalmic Center, Sun Yat-sen University, P.R. China. The print version of this article was created on 25 March 2024. This reflects all typographical corrections and errata to the article through that date. Details of any changes may be found in the online version of the article.